NASA TECHNICAL NOTE

FLIGHT- AND GROUND-TEST EVALUATION OF PYRRONE FOAMS

by Allen G. McLain and Warren C. Kelliher

Langley Research Center
Hampton, Va. 23365

NATIONAL AERONAUTICS AND SPACE ADMINISTRATION • WASHINGTON, D. C. • MARCH 1972

1. Report No. NASA TN D-6711	2. Government Accession No.	3. Recipient's Catalog No.
4. Title and Subtitle FLIGHT- AND GROUND-TEST EVALUATION OF PYRRONE FOAMS		5. Report Date March 1972 6. Performing Organization Code
7. Author(s) Allen G. McLain and Warren C. Kelliher		8. Performing Organization Report No. L-8100
9. Performing Organization Name and Address NASA Langley Research Center Hampton, Va. 23365		10. Work Unit No. 970-32-20-13 11. Contract or Grant No.
12. Sponsoring Agency Name and Address National Aeronautics and Space Administration Washington, D.C. 20546		13. Type of Report and Period Covered Technical Note 14. Sponsoring Agency Code
15. Supplementary Notes		

16. Abstract

Two Pyrrone materials, pure Pyrrone foam with a density of 481 kg/m^3 and hollow-glass-microsphere—Pyrrone composite with a density of 962 kg/m^3, were tested in the Langley 20-inch hypersonic arc-heated tunnel at pressure levels from 0.06 to 0.27 atm (1 atm = 101.3 kN/m^2) and heating rates from 1.14 to 11.4 MW/m^2. The 481-kg/m^3 Pyrrone foam was also flight tested as an experiment aboard a Pacemaker test vehicle. The results of the ground tests indicated that the thermal effectiveness of the 481-kg/m^3 Pyrrone foam was superior to the 962-kg/m^3 glass-sphere—Pyrrone composite. The 481-kg/m^3 Pyrrone foam had approximately one-half the thermal effectiveness of low-density phenolic nylon. The 481-kg/m^3 Pyrrone foam experienced random mechanical char removal over the entire range of test conditions. Char thermal-property inputs for an ablation computer program were developed from the ground-test data of the 481-kg/m^3 Pyrrone foam. The computer program using these developed char thermal properties, as well as the measured uncharred material properties, adequately predicted the in-depth temperature histories measured during the Pacemaker flight.

17. Key Words (Suggested by Author(s)) Ablation Pyrrone	18. Distribution Statement Unclassified – Unlimited

19. Security Classif. (of this report) Unclassified	20. Security Classif. (of this page) Unclassified	21. No. of Pages 32	22. Price* $3.00

*For sale by the National Technical Information Service, Springfield, Virginia 22151

FLIGHT- AND GROUND-TEST EVALUATION OF PYRRONE FOAMS

By Allen G. McLain and Warren C. Kelliher
Langley Research Center

SUMMARY

Two Pyrrone materials, pure Pyrrone foam with a density of 481 kg/m^3 and hollow-glass-microsphere—Pyrrone composite with a density of 962 kg/m^3, were tested in the Langley 20-inch hypersonic arc-heated tunnel at pressure levels from 0.06 to 0.27 atm (1 atm = 101.3 kN/m^2) and heating rates from 1.14 to 11.4 MW/m^2. The 481-kg/m^3 Pyrrone foam was also flight tested as an experiment aboard a Pacemaker test vehicle. The results of the ground tests indicated that the thermal effectiveness of the 481-kg/m^3 Pyrrone foam was superior to the 962-kg/m^3 glass-sphere—Pyrrone composite. The 481-kg/m^3 Pyrrone foam had approximately one-half the thermal effectiveness of low-density phenolic nylon. The 481-kg/m^3 Pyrrone foam experienced random mechanical char removal over the entire range of test conditions. Char thermal-property inputs for an ablation computer program were developed from the ground-test data of the 481-kg/m^3 Pyrrone foam. The computer program using these developed char thermal properties, as well as the measured uncharred material properties, adequately predicted the in-depth temperature histories measured during the Pacemaker flight.

INTRODUCTION

The low-density, char-forming, ablative materials presently used for heat shields are mixtures of various fillers held together by a polymeric resin. A typical example is low-density phenolic nylon. The filler materials usually enhance certain aspects of the ablative process, lower the composite density, and enhance structure, while the basic resin provides the char structure.

The Pyrrones (polyimidazopyrrolones, ref. 1) are a new class of polymers developed at Langley Research Center for use in high-temperature environments. Test specimens having densities in the range of presently used charring ablators were fabricated by using the Pyrrone-base resin for a series of ground ablation tests. Chemical foaming of the Pyrrone resins and addition of hollow glass microspheres were found to be the two best methods to reduce the density of the Pyrrones. These methods resulted in a pure Pyrrone

foam (P30) with a density of 481 kg/m^3 and a hollow-glass-microsphere—Pyrrone composite (P60) with a density of 962 kg/m^3.

An investigation was initiated to compare the ablative performance of both the P30 and P60 materials with existing ablative materials of comparable densities. These tests were carried out in the Langley 20-inch hypersonic arc-heated tunnel at pressure levels from 0.06 to 0.27 atm and heating rates from 1.14 to 11.4 MW/m^2. The data from these tests included the measurement of internal temperatures, surface temperatures, and surface recessions.

The P30 material was also flown aboard a Pacemaker test vehicle to determine its ablative behavior in a flight environment.

The ground- and flight-test data were compared with analytical predictions; the data and the comparisons are presented herein.

SYMBOLS

B	preexponential for decomposition (see table 6), per sec
B_m	preexponential for surface-oxidation kinetics (see ref. 12)
c_p	heat capacity, J/kg-K
E/R	activation energy for decomposition divided by universal gas constant, K (see table 6)
E_m	activation energy for surface oxidation kinetics, J/mole
h	enthalpy, J/kg
k	adjusted thermal conductivity, W/m-K
ΔL	recession, meters
p	pressure, atm (1 atm = 101.3 kN/m^2)
Q_T	total cold-wall heat input, J/m^2
$\dot{q}$	cold-wall heating rate, W/m^2

r_{eff} effective hemispherical nose radius, meters

T temperature, K

T_s surface temperature, K

$t_{\Delta T}$ time for 167 K temperature rise, seconds

w unit mass, kg/m^2

ϵ emissivity

ρ_o density of reactants, kg/m^3 (see table 6)

ρ_R density of residue, kg/m^3 (see table 6)

τ shear, N/m^2

ψ reaction order (see table 6)

Subscripts:

l local

max maximum

t stagnation point

SYNTHESIS AND PRODUCTION OF PYRRONE FOAMS

The Pyrrone polymer is a thermosetting resin resulting from the reaction of an aromatic tetraamine with an aromatic dianhydride. (See ref. 1.) The prepolymerization is carried out in aprotic solvents to form an amide-acid-amine prepolymer, which is then fabricated into a desired shape and thermally cured to the fully cyclized polymer. Considerable difficulty was experienced in fabricating materials from the prepolymers prepared by this process. (See ref. 2.) Subsequently, the prepolymer stage was prepared by first esterifying the dianhydride and reacting the ester with the tetraamine to form an amide-ester-amine prepolymer. (See fig. 1.) This prepolymer stage is easy to process into fabricated shapes and is particularly useful in producing high-strength foams.

(See ref. 3.) By using various diols or alcohols as the esterifying agent, a variety of intermediate resins can be produced, each individually suited for fabricating either chemically blown foams or syntactic foams.

P30 Material

Benzophenone tetracarboxylic dianhydride (BTDA) was reacted with ethyl alcohol to form a molten tetraester monomer to which was added solid diaminobenzidine (DAB) to form a prepolymer resin. (See fig. 1.) This material, which has a melting point of 383 K to 393 K, was mixed with a chemical blowing agent and used as the basic molding resin. This resin was preformed in a ram mold at a pressure of 34.5 MN/m^2, then the ram mold was raised and clamped to the desired foam thickness. The mold assembly was then heated to 408 K, during which time the resin expanded to fill the mold cavity, kept at that temperature for 5 hours, and then temperature programed at a constant rate from 408 K to 583 K over a 5-hour period. After cooling to room temperature, the foam was removed from the mold and postcured in argon from 422 K to 644 K over a 5-day period.

The mechanical and thermal properties of the P30 foam are given in table 1. The cell sizes of the foam vary from 0.02 to 0.05 cm, and the cells are uniformly distributed throughout. (See fig. 2.) Although from the photograph the foam appears to be closed cell, the value of the volume fraction of continuous voids indicates that it is essentially an open-cell foam.

P60 Material

Benzophenone tetracarboxylic dianhydride (BTDA) was esterified with ethylene glycol to form a tetraester monomer. (See fig. 1.) Excess ethylene glycol was used so that the subsequent addition of solid DAB monomer would result in a solution polymerization to form a prepolymer resin. The prepolymer was precipitated with water, washed, and dried. Thirty percent by weight of hollow glass microspheres was added to the powdered precipitate, and this mixture was used as the basic resin. This molding resin was placed in a mold and compressed to the desired foam thickness. The mold assembly was heated to 422 K, and the temperature was increased at a constant rate from 422 K to 589 K over a 6-hour period. After cooling to room temperature, the foam was removed from the mold and postcured in argon at a temperature from 422 K to 644 K over a 5-day period.

The mechanical and thermal properties of the P60 foam are also given in table 1. Examination of cross sections of the P60 foam showed only a small amount of breakage of the hollow glass microspheres, which indicates that the resin flowed sufficiently during cure to produce a uniform hydrostatic pressure on the glass microspheres.

TEST PROCEDURE

Flight Test

The P30 material was flown aboard a Pacemaker test vehicle as a secondary experiment to determine its ablative behavior in a flight environment. The primary experiment aboard the Pacemaker was an ablative test of a carbon-phenolic material. The results of the primary experiment are presented in reference 4. Pertinent information on the telemetry and vehicle operations, which applies to both the primary and secondary experiments, can also be found in reference 4.

Test panel location and instrumentation.- The P30 material panels were located on the cylindrical section of the Pacemaker test vehicle. The precise location of the panels may be seen in figure 3. The panels were each 36.18 cm in length with an outer radius of 12.70 cm and an inner radius of 11.72 cm. (See fig. 4.) Each panel covered 60^{o} of the cylindrical section. Instrumentation, consisting of two chromel/alumel thermocouples and two chromel/constantan thermocouples, was located at station G-G' in figure 3. Three of the thermocouples were positioned in depth in the panel designated P11. The remaining thermocouple was positioned in depth in the panel designated P8. The panel designations are shown in figure 4. The thermocouples were in plugs which were pushed into holes drilled from the inside of the cylinder to the proper depth from the outside surface. The arrangement of the plugs in the panels can be seen in figure 4. The distances from the outer surface to the thermocouples in panel P11 were 0.33, 0.66, and 0.94 cm. The distance from the surface to the thermocouple in panel P8 was 1.02 cm. This thermocouple was located beneath a 0.08-cm thickness bond line of silicone-rubber adhesive.

The P30 material panels were bonded to a layer of phenolic cork 0.635 cm thick by an elastomeric silicone-rubber adhesive, which, in turn, was bonded to the aluminum substructure of the spacecraft with an epoxy adhesive. The silicone-rubber adhesive was also used as a bond between the different panels located on the cylindrical section and between the panels and the primary material tested during the flight.

Flight-test environment.- The ambient pressure and temperatures of the atmosphere in the launch vicinity were measured just prior to the launch by a rawinsonde as indicated in reference 4. From these measurements, values of ambient atmospheric density were computed and presented in reference 4.

Computed pressure distributions over the cylindrical section of the test vehicle are presented in reference 4 for several free-stream Mach numbers. Computed time histories of local cold-wall heating rates based on computed pressures, local recovery enthalpies, local pressures, and local turbulent shears are presented in figures 5 to 8, respec-

tively. These computations were made for the actual flight trajectory using the method described in reference 4.

Ground Tests

Model assembly.- In figure 9 the dimensions of each of the three different size models are shown. The particular nose shape was chosen to ensure constant heating rates over a major part of the forward surface of the models. The models consisted of the P30 material or P60 material machined to one of the three sets of dimensions indicated in figure 9. A thermocouple plug of the P30 or P60 material (shown also in fig. 9) with thermocouples installed was bonded into the Pyrrone model with a Pyrrone adhesive. The assembled model was then bonded to a canvas-reinforced phenolic-sting adapter with a silicone-rubber adhesive. A typical model is shown disassembled in figure 10, illustrating the Pyrrone model, thermocouple plug, and the sting adapter and sting.

Three thermocouples were located in the P30 models nominally 0.381, 0.813, and 1.18 cm from the outer surface on the model center line. In all but three of the P30 models, the thermocouple nearest the surface was 36-gage platinum/platinum-13% rhodium. For these three which were to be used specifically for the Pacemaker flight comparisons, the thermocouple was 36-gage chromel/alumel. The remaining two thermocouples in all of the P30 models were 30-gage chromel/alumel. The lead wires of the thermocouple nearest the surface, in all the models, were insulated by alumina tubes which were press fitted into slots along the sides of the thermocouple plug. The lead wires of the remaining thermocouples were insulated by polyethylene tubing.

Three thermocouples were also located in the P60 models nominally 0.406, 0.591, and 1.016 cm from the outer surface. Four additional P60 models were constructed with thermocouples located 0.191, 0.406, and 0.591 cm from the outer surface. The thermocouple nearest the surface in all of the P60 models was 36-gage platinum/platinum-13% rhodium and was insulated with alumina tubing. The remaining thermocouples were 30-gage chromel/alumel with polyethylene tubing for insulation.

Test conditions.- The pressure levels, heating rates, and enthalpies for the ground tests are listed in table 2. The special Pacemaker test conditions are presented in table 3. The stagnation-point pressure and heating rate were measured prior to the insertion of the models into the test stream. The heating rates were measured with a thin-wall flat-face calorimeter 2.54 cm in diameter. The heating rates were converted to the heating rate for the particular model shape by the method presented in reference 5. The enthalpies were calculated from the measured heating rates using the empirical correlation of reference 6.

Special Pacemaker tests.- Three P30 models were ground tested specifically in support of a Pacemaker flight test. These tests were conducted to simulate the expected

environment for the P30 panels during the flight. The exposure time of each model to the simulated environment was based on the expected preflight total cold-wall heat input to the Pyrrone panel at the instrumentation location. The stagnation-point heating rates, enthalpies, pressures, and peak corner shears for the special ground tests are compared with the conditions at peak heating at the flight-panel instrument location for the actual flight trajectory in figures 5 to 8, respectively. The comparative total cold-wall heat inputs to the ground-test models and the flight panels are shown in figure 5. The peak corner shears for the ground-test models shown in figure 8 were calculated by using the approximate method of reference 7.

RESULTS AND DISCUSSION

Ground Tests

The ground-test results are summarized in tables 3, 4, and 5.

Thermal effectiveness.- Thermal-effectiveness values in MJ/kg were calculated for the models as defined by

$$\text{Thermal effectiveness} = \frac{(\dot{q})(t_{\Delta T})}{w}$$

where $\dot{q}$ is the cold-wall heating rate to the model, $t_{\Delta T}$ is the time required for a temperature rise of 167 K, and w is the unit mass of ablation material. These values are listed in table 4 for several different unit masses over a range of different pressure levels and heating rates, as indicated for each test on table 2.

A comparison was made between the thermal-effectiveness values for the P30 and P60 materials over a similar heating-rate range. This comparison is shown in figure 11 for a unit weight of approximately 3.9 kg/m^2. As can be seen, the values of thermal effectiveness for the P30 material fall above those for the P60 material by a factor of approximately two. This comparison illustrates the lower insulation ability for the P60 material. The effect of the stagnation-point pressure on the thermal-effectiveness values of the two materials can also be seen in figure 11. At the two different pressure levels of the tests, approximately 0.06 and 0.27 atm, the thermal-effectiveness values for the P60 material fall along the same line. The thermal-effectiveness values for the P30 material for the two different pressure levels fall along two different lines. (The lines in fig. 11 do not represent a fit of the data but are used merely as aids in observing this difference.) The variation in thermal-effectiveness values for the P30 material with pressure might be attributed to the highly porous nature of the material; this characteristic may allow internal flow of hot gases.

In figure 12 the thermal-effectiveness values of the P30 material are compared with the data for low-density phenolic nylon (LDPN) from reference 8. The unit weight of the

low-density phenolic nylon was 1.83 kg/m^2, and the P30 material had unit masses varying between 1.66 and 1.91 kg/m^2. As can be seen in this figure, the data points for the two different materials are almost parallel. The P30 material, however, exhibited thermal-effectiveness values roughly one-half those for low-density phenolic nylon material. This difference is thought to be due to the pressure difference in the two series of tests.

However, as shown in figure 13, the same thermal-effectiveness values for the P30 material are compared with thermal-effectiveness values derived from data at similar pressure levels in reference 9 for two other formulations of low-density phenolic nylon. The thermal-effectiveness values from the data of reference 9 resulted in unit mass lines shown in figure 13. For the lower line, the unit masses ranged from 1.31 to 1.72 kg/m^2. The unit masses for the upper line ranged from 2.86 to 3.26 kg/m^2. Again the thermal-effectiveness values for the P30 material are approximately one-half those for the low-density phenolic nylon. (In this figure the lines are placed merely to help distinguish between the two different ranges of unit masses of the low-density phenolic nylon.)

The comparisons of thermal-effectiveness values of the P30 material with those of low-density phenolic nylon from references 8 and 9 indicate the two types of Pyrrone foams have lower effective insulative properties than the low-density phenolic nylon. This result is probably due to the high porosity of the Pyrrone foams and their high decomposition temperature and high char yield. The high porosity of the foams could allow the hot gases from the arc-jet tests to flow into the foam material causing a fast back-surface temperature rise and thus a low value of thermal effectiveness. The high decomposition temperature and high percentage char yield of the Pyrrone resin causes the material to have a smaller amount of gaseous products during decomposition than the phenolic nylon.

Surface recession.- The surface-recession data and surface temperatures for the ground test are presented in table 5 for the P30 and P60 materials. Although the P30 material retained approximately the same model shape and relatively smooth surface during testing, examination of the high-speed motion-picture film taken during the tests showed particles of char leaving the surface.

The P60 material models also retained the original model shape and a smooth surface during testing; however, the motion-picture films indicated that molten glass on the surface flowed to the corners and was sheared from the model into the airstream.

Ablation Model Inputs

The ground-test data were used to develop inputs to the Aerotherm Corporation charring-material-ablation computer program (CMA) described in reference 10, which would describe the ablative behavior of the P30 material. The material properties in table 1 were used as inputs to the computer program for the uncharred Pyrrone material. The char properties, thermal conductivity and specific heat, were not measured. The

required inputs were obtained as follows: Char-layer specific heat was assumed to be in the range of values measured for other ablation-material chars; the temperature variation of thermal conductivity of the Pyrrone char was assumed to be similar to that of low-density phenolic-nylon char measured in reference 11; and the thermal-conductivity values were adjusted to produce good agreement with the ground-test results. Table 6 contains the final char thermal-conductivity variation with temperature, the assumed char specific-heat variation with temperature, and the constants needed by the CMA to calculate uncharred material decomposition. The material-decomposition reactions listed in table 6(a) were obtained from unpublished thermogravimetric-analysis data.

The Aerotherm Corporation chemical-equilibrium computer program (ACE), described in reference 12, was used to calculate chemical reactions at the char surface. The elemental analysis of the P30 material, given in table 1, and the assumption of a pure carbon char afforded the necessary inputs for the ACE computer program.

The computer inputs developed from the data of the tests at 0.066 and 0.27 atm were used to predict the ablative response for comparison with the three models specifically tested in support of the Pacemaker flight test of the P30 material. The only change in the computer model for these comparisons was the use of rate constants in the ACE computer program to describe the oxidation of the carbon surface. The values for the activation energy E_m and the preexponential B_m for the surface oxidation kinetics are 137 kJ/mole and 6700 moles of reactant/m^2-sec-atm, respectively. The comparisons are shown in figures 14 to 16. A possible 0.05-cm uncertainty in the actual thermocouple location within the test model is indicated.

The values of measured and computed surface recessions are listed in table 7. The models did lose some solid particles from the surface during the tests; however, the computer model only considered oxidation. The forward surfaces of the models may be seen in figure 17. The models remained fairly smooth and retained the original shape very well. The surface of the largest diameter model appears to have had some large voids near the corners, which became exposed after the test. The pyrolysis zone of the three models can be observed in figure 17. The transition from uncharred material to char is sharply defined. The pyrolysis depth measured to the sharply defined interface is given for each of the models in table 7. For the CMA program pyrolysis-zone depths are given at points within 2 percent of the final char density and within 98 percent of uncharred material density. In test 1 the two computed values bracketed the measured value. For tests 2 and 3, however, the measured values fall closer to the values at 98 percent of uncharred material density.

The computed surface temperatures shown in figures 14 to 16 were approximately 10 to 20 percent lower than the experimentally measured surface temperatures. Com-

puted surface temperatures using the different ablation programs available have usually been lower than the temperatures measured with the photographic optical pyrometer. (See, for example, ref. 13.)

Flight Test

The telemetered temperature histories for the three thermocouples in panel P11 and the one thermocouple in panel P8 are shown in figure 18. The temperature histories shown in figure 18 and designated P11-1, P11-2, and P11-3 were measured at 0.33, 0.66, and 0.94 cm from the outer surface, respectively. The temperature history shown in figure 18 and designated P8-1 was recorded by the thermocouple at a depth of approximately 1.02 cm from the outer surface.

The computer model developed from the ground-test data was used to calculate data for a comparison with the flight-test results. The comparison between the experimental and computed temperature histories is quite good, as shown in figure 19. A possible 0.05-cm uncertainty in actual thermocouple location in the test model is indicated. The region past 100 seconds indicated that the computed temperature histories tended to diverge from the experimental data, as was observed in the ground-test results.

The surface recession along the axial center line during the flight is shown in figures 20 and 21. Measurements were also taken approximately 18° to either side of the panel center line. Figure 20 shows the surface recession of panel P11, and figure 21 shows the surface recession of panel P8. Recession calculations were made only for the panel-instrument locations at the panel center line. The closed symbol in figures 20 and 21 at the axial distance of 53.01 cm represents the computed surface recession. The computed surface recession fell within range of the measured surface recession for panel P11. For panel P8, however, the computed surface recession was approximately one-third lower than that measured. The discrepancy between the surface recessions indicated for panel P11 and panel P8 may be attributed in part to postflight handling. It is known that some of the char had to purposely be removed because of radioactive contamination from a radioactive ablation sensor located at the stagnation point of the test vehicle.

The appearance of the char was very similar to that formed during the ground tests. The remaining char on the test-vehicle panels was slightly rougher than the char on the ground-test models – possibly because of the postflight handling of the panels. In figure 22 panel P11 is shown after sectioning along the center line. The panel surface, center-line profile, and a closeup of the thermocouple plug are shown. More char was lost during the sectioning, and it appears in the photograph that the thermocouple is on the surface. In figure 23, panel P8 is shown in the same manner. A closeup of the

thermocouple plug indicates the 0.08 cm of silicone rubber bond line between the Pyrrone material and the thermocouple.

Determination of the interface between the char and the uncharred Pyrrone was difficult, unlike the ground tests, primarily because of the dark color of the pure Pyrrone foam and its similarity in texture to its char. Based on the measured internal temperatures and the known decomposition temperature the interface would have to be located between the thermocouples at 0.33 and 0.66 cm from the outer surface. The calculated pyrolysis zone (interface) was located 0.43 cm below the original outer surface. There does not appear to be an abrupt change in material hardness or appearance between two thermocouples in the flight panel.

CONCLUDING REMARKS

Two Pyrrone resin-based ablation materials, pure Pyrrone foam (P30) with a density of 481 kg/m^3 and hollow-glass-microsphere—Pyrrone composite (P60) with a density of 962 kg/m^3, were tested in the Langley 20-inch hypersonic arc-heated tunnel at pressure levels from 0.06 to 0.27 atm (1 atm = 101.3 kN/m^2) and heating rates from 1.14 to 11.4 MW/m^2. The 481-kg/m^3 Pyrrone foam was flight tested as the secondary experiment aboard the Pacemaker test vehicle described in NASA TM X-2504.

By using thermal-effectiveness values calculated from in-depth temperature measurements in ground-test models, comparisons were made between the P30 and P60 materials and between the P30 material and the low-density phenolic nylons reported in NASA TN D-1889 and NASA CR-1207. The P60 material exhibited thermal-effectiveness values roughly one-half those for the P30 material. The latter exhibited thermal-effectiveness values roughly one-half of those for low-density phenolic nylon. However, it should be pointed out that the Pyrrone foam unlike the low-density phenolic nylons does not contain any additive to enhance its ablative performance.

The P30 material, experienced particulate char removal at all of the ground-test conditions used in this investigation.

The computer inputs developed from the ground-test data of the P30 material adequately predicted the in-depth temperature histories measured during the Pacemaker flight.

Langley Research Center,
National Aeronautics and Space Administration,
Hampton, Va., March 1, 1972.

REFERENCES

1. Pezdirtz, George F.; and Bell, Vernon L.: An Exploratory Study of a New Class of Stepladder and Ladder Polymers – Polyimidazopyrrolones. NASA TN D-3148, 1965.

2. Karre, L. E.; Keller, L. B.; and Miller, L. J.: Development and Processing of Pyrrone Polymers. NASA CR-1310, 1969.

3. Kimmel, B. G.; and Karre, L. E.: Preparation and Characterization of the Pyrrones as Thermal Structural Materials. Rep. No. P69-112 (Contract No. NAS 1-7381), Aerospace Group, Hughes Aircraft Co., 1968. (Available as NASA CR-66853.)

4. Walton, Thomas E., Jr.; and Witte, William G.: Flight Test of Carbon-Phenolic on a Spacecraft Launched by the Pacemaker Vehicle System. NASA TM X-2504, 1972.

5. Zoby, Ernest V.; and Sullivan, Edward M.: Effects of Corner Radius on Stagnation-Point Velocity Gradients on Blunt Axisymmetric Bodies. NASA TM X-1067, 1965.

6. Zoby, Ernest V.: Empirical Stagnation-Point Heat-Transfer Relation in Several Gas Mixtures at High Enthalpy Levels. NASA TN D-4799, 1968.

7. Zoby, Ernest V.: Approximate Relations for Laminar Heat-Transfer and Shear-Stress Functions in Equilibrium Dissociated Air. NASA TN D-4484, 1968.

8. Vojvodich, Nick S.; and Winkler, Ernest L.: The Influence of Heating Rate and Test Stream Oxygen Content on the Insulation Efficiency of Charring Materials. NASA TN D-1889, 1963.

9. Hiester, Nevin K.; and Clark, Carroll F.: Comparative Evaluation of Ablating Materials in Arc Plasma Jet. NASA CR-1207, 1968.

10. Moyer, Carl B.; and Rindal, Roald A.: An Analysis of the Coupled Chemically Reacting Boundary Layer and Charring Ablator. Part II. Finite Difference Solution of the In-Depth Response of Charring Materials Considering Surface Chemical and Energy Balances. NASA CR-1061, 1968.

11. Engelke, W. T.; Pyron, C. M., Jr.; and Pears, C. D.: Thermophysical Properties of a Low-Density Phenolic-Nylon Ablation Material. NASA CR-809, 1967.

12. Kendall, Robert M.: An Analysis of the Coupled Chemically Reacting Boundary Layer and Charring Ablator. Pt. V – A General Approach to the Thermochemical Solution of Mixed Equilibrium-Nonequilibrium, Homogeneous or Heterogeneous Systems. NASA CR-1064, 1968.

13. McLain, Allen G.; Sutton, Kenneth; and Walberg, Gerald D.: Experimental and Theoretical Investigation of the Ablative Performance of Five Phenolic-Nylon-Based Materials. NASA TN D-4374, 1968.

TABLE 1.- PROPERTIES OF PYRRONE FOAMS

[Chemical composition by weight: 76.1% C, 7.2% H, 4.8% N, 11.9% O]

Property	P30	P60
Compressive strength, MN/m^2 (ASTM Method D 695-69):		
At 298 K	10.3	27.8
At 644 K	10.3	23.9
Tensile strength, MN/m^2 (ASTM Method D 651-48):		
At 298 K	4.2	8.4
At 644 K	1.9	5.4
Volume fraction of continuous voids (impregnation procedure)	0.66	0.36
Thermal conductivity, W/m-K (Cenco-Fitch procedure)	0.096	0.222
Specific heat, J/kg-K (calorimetric procedure)	1130	1130

TABLE 2.- GROUND-TEST CONDITIONS

Test	P30			P60		
	p_t, atm	$\dot{q}$, MW/m^2	h_t, MJ/kg	p_t, atm	$\dot{q}$, MW/m^2	h_t, MJ/kg
1	0.063	1.19	8.09	0.061	1.88	14.78
2	.060	1.28	10.20	.061	2.09	14.16
3	.061	1.79	14.03	.066	2.98	22.25
4	.061	2.26	15.33	.066	3.44	22.25
5	.066	2.88	21.60	.268	2.33	8.83
6	.061	2.88	15.97	.256	2.72	9.15
7	.066	3.30	21.38	.261	2.48	9.50
8	.066	4.56	24.10	.266	2.66	8.83
9	.261	2.32	8.89	.250	2.70	9.16
10	.268	2.33	8.83	.266	2.82	9.27
11	.261	2.48	9.50	.266	2.82	9.27
12	.266	2.66	8.83	.264	3.45	9.30
13	.250	2.70	9.16	.214	3.64	10.89
14	.256	2.72	9.15	.234	5.25	20.85
15	.264	3.45	9.30	.260	5.31	20.00
16	.214	3.64	10.89	.263	5.28	19.50
17	.263	5.28	19.50	.256	5.71	18.80
18	.260	5.31	20.00	.224	6.05	21.23
19	.256	5.71	18.80	.250	6.59	21.90
20	.224	6.05	21.23	.238	8.02	22.30
21	.250	6.59	21.90	.250	8.08	21.90
22	.250	8.08	21.90	.250	8.55	23.22
23	.250	8.55	23.22			
24	.250	11.60	31.30			

TABLE 3.- SPECIAL PACEMAKER GROUND-TEST DATA

FOR P30 MATERIAL

Characteristic	Test 1	Test 2	Test 3
p_t, atm	0.240	0.240	0.247
$\dot{q}$, MW/m^2	1.32	1.28	1.48
h_t, MJ/kg	6.01	5.08	4.78
r_{eff}, cm	5.53	4.15	2.77
ΔL, cm	0.095	0.165	0.173
Time, sec	14.8	17.3	14.8
T_s, K	2170	2250	2300
Thermal effectiveness at $w = 1.83$ kg/m^2, MJ/kg	5.33	4.18	4.68

TABLE 4.- THERMAL EFFECTIVENESS AT VARIOUS UNIT WEIGHTS FOR BOTH P30 AND P60 MATERIALS

Test	Thermal effectiveness at 167 K, MJ/kg, for –						
	P30 at w, kg/m^2, of –			P60 at w, kg/m^2, of –			
	1.66 to 1.91	3.71 to 4.00	5.66 to 5.81	1.85	3.92	5.71	9.91
1	4.52	7.41	9.86	3.58	5.77	----	----
2	4.36	8.50	10.57	3.61	5.88	----	----
3	6.28	11.20	14.05	4.34	8.00	----	----
4	6.58	11.62	15.10	5.70	7.38	----	----
5	8.46	----	----	---	6.54	8.00	----
6	8.19	13.50	17.05	---	6.16	----	----
7	7.63	14.12	----	---	5.86	8.05	11.50
8	10.50	19.10	----	---	6.45	8.44	----
9	6.09	9.16	10.55	---	6.86	8.53	----
10	5.95	----	----	---	6.43	8.90	----
11	6.88	11.54	----	---	7.70	9.27	12.44
12	6.51	----	----	---	9.12	10.65	----
13	6.80	9.45	----	---	9.40	11.58	14.30
14	7.85	10.56	12.78	---	12.20	----	----
15	----	----	----	---	11.10	----	----
16	8.86	12.60	14.00	---	11.38	----	20.30
17	9.73	16.99	----	---	11.88	15.32	----
18	----	----	----	---	13.13	16.93	22.15
19	10.48	16.60	----	---	13.80	----	----
20	----	----	----	---	18.32	----	----
21	12.04	----	----	---	16.60	----	----
22	----	21.18	----	---	----	18.25	32.50
23	15.60	22.58	24.00				
24	18.30	28.24	32.80				

TABLE 5.- MEASURED SURFACE TEMPERATURES AND RECESSIONS

Test	P30					P60				
	p_t, atm	ΔL, cm	Time, sec	T_s, K	r_{eff}, cm	p_t, atm	ΔL, cm	Time, sec	T_s, K	r_{eff}, cm
1	0.063	0.284	47.3	2220	4.15	0.061	0.074	23.2	2250	5.53
2	.060	.287	47.5	2220	5.53	.061	.097	21.6	2280	4.15
3	.061	.244	44.8	2360	5.53	.066	.086	21.6	2460	5.53
4	.061	.259	37.8	2500	4.15	.066	.162	20.2	2660	4.15
5	.066	.160	30.2	2650	5.53	.268	.457	44.0	2390	5.53
6	.061	.338	34.2	2600	2.77	.256	.193	22.0	2390	5.53
7	.066	.252	32.6	2760	4.15	.261	.670	64.2	2390	5.53
8	.066	.320	28.3	2810	2.77	.266	.515	39.0	2440	4.15
9	.261	.430	28.0	2750	5.53	.250	.706	59.2	2440	4.15
10	.268	.058	9.0	2750	5.53	.266	.251	20.0	2470	4.15
11	.261	.254	19.0	2750	5.53	.266	.713	59.0	2470	4.15
12	.266	.122	10.0	2810	4.15	.264	.417	26.0	----	2.77
13	.250	.353	18.0	2810	4.15	.214	.752	52.0	----	2.77
14	.256	.513	27.2	2810	4.15	.234	.239	20.0	2840	5.53
15	.264	.256	12.0	3000	2.77	.260	.475	35.0	2750	5.53
16	.214	.548	22.5	3000	2.77	.263	.726	50.6	2890	5.53
17	.263	.412	24.0	3190	5.53	.256	.410	24.0	2780	4.15
18	.260	.244	17.0	3190	5.53	.224	.595	35.6	2860	4.15
19	.256	.323	17.0	3250	4.15	.250	.211	13.0	2840	4.15
20	.224	.389	23.0	3250	4.15	.238	.300	12.0	2840	2.77
21	.250	.127	9.0	3250	4.15	.250	.585	25.0	2920	2.77
22	.250	.310	11.0	3470	2.77	.250	.856	39.0	3140	2.77
23	.250	.581	17.4	3470	2.77					
24	.250	.541	16.4	3550	2.77					

TABLE 6.- INPUTS TO CHARRING-MATERIAL-ABLATION COMPUTER PROGRAM FOR CHARRED P30 MATERIAL

(a) Constants for decomposition reactions

Constant	Reaction A	Reaction B
ρ_O, kg/m^3	63	418
ρ_R, kg/m^3	0	338 (final char density)
E/R, K	12 830	17 300
B, sec^{-1}	2.300×10^4	3.333×10^5
ψ	1.25	1.89

(b) Char thermophysical properties

T, K	ϵ	c_p, J/kg-K	k, W/m-K
278	0.88	3340	0.468
556	↓	3350	.468
666	↓	↓	.405
723	↓	↓	.280
778	↓	↓	.218
834	↓	↓	.187
890	↓	↓	.187
945	↓	↓	.187
1000	↓	↓	.250
1110	↓	↓	.900
1390	↓	↓	2.500
2780	↓	↓	10.500

TABLE 7.- MEASURED AND COMPUTED RECESSION OF SURFACE AND OF INTERFACE BETWEEN CHAR AND UNCHARRED MATERIAL FOR SPECIAL PACEMAKER TESTS

Test	Surface recession, cm		Char-uncharred interface recession, cm		
				Computed	
	Measured	Computed	Measured	2% char density	98% uncharred density
1	0.096	0.124	0.445	0.136	0.531
2	.165	.166	.597	.188	.595
3	.173	.203	.612	.220	.602

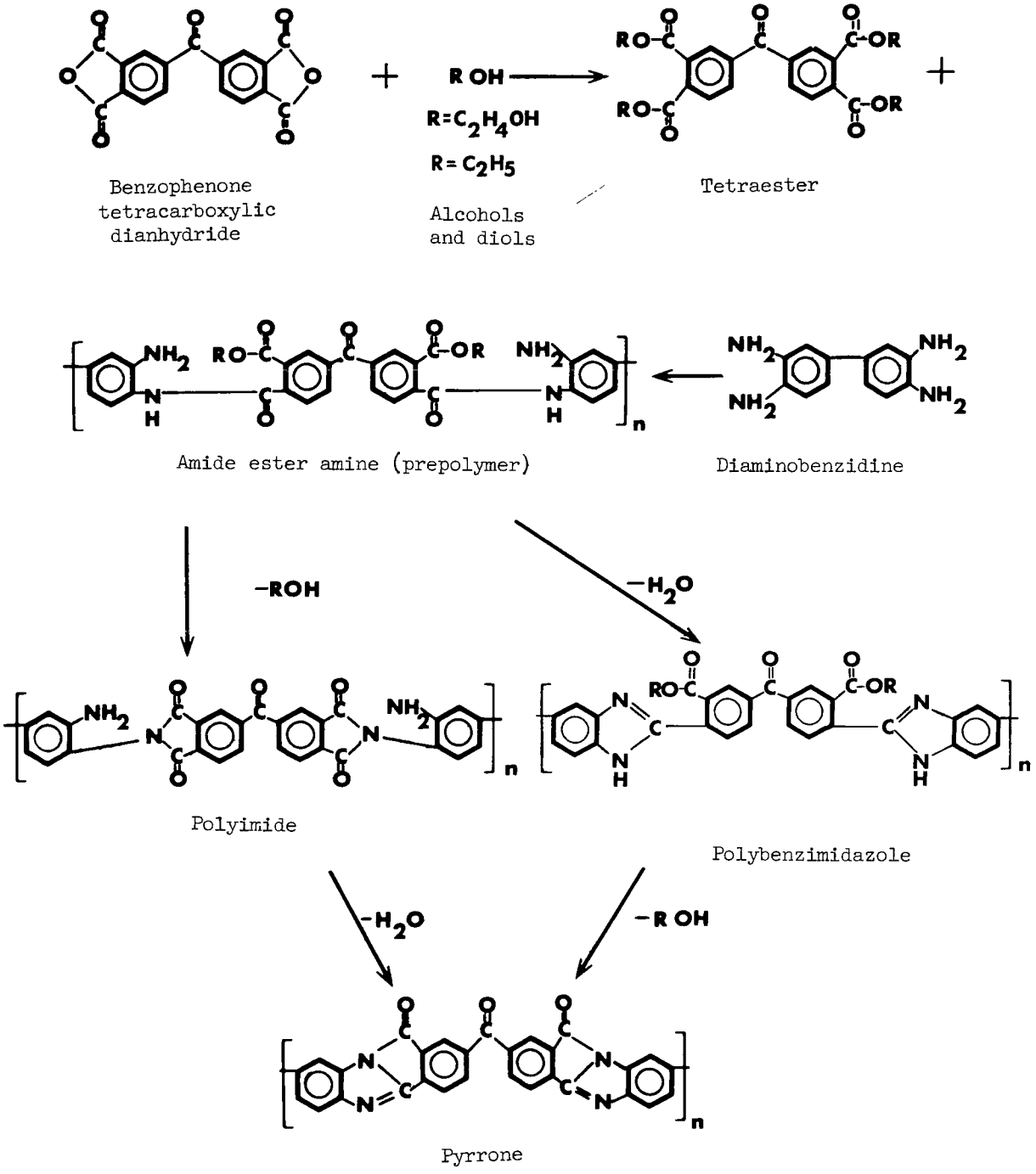

Figure 1.- Synthesis of Pyrrone resins for production of foams.

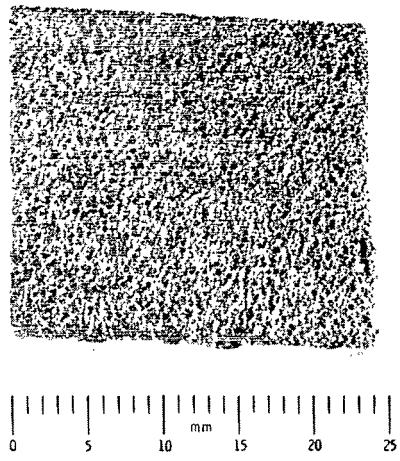

L-72-141

Figure 2.- Cross section of 481-kg/m^3 pure Pyrrone foam.

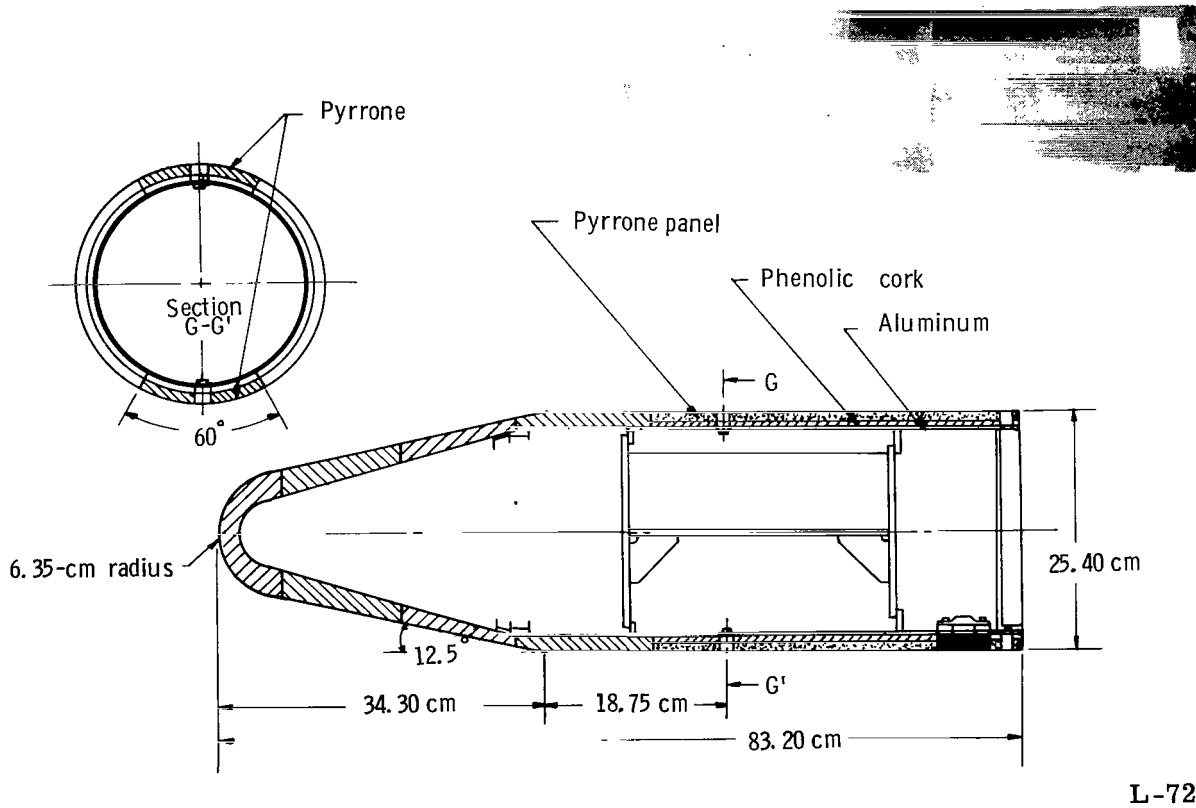

L-72-142

Figure 3.- Sectioned view of Pacemaker test vehicle illustrating the P30 material panel and instrumentation location. (Photograph of test vehicle in upper right-hand corner.)

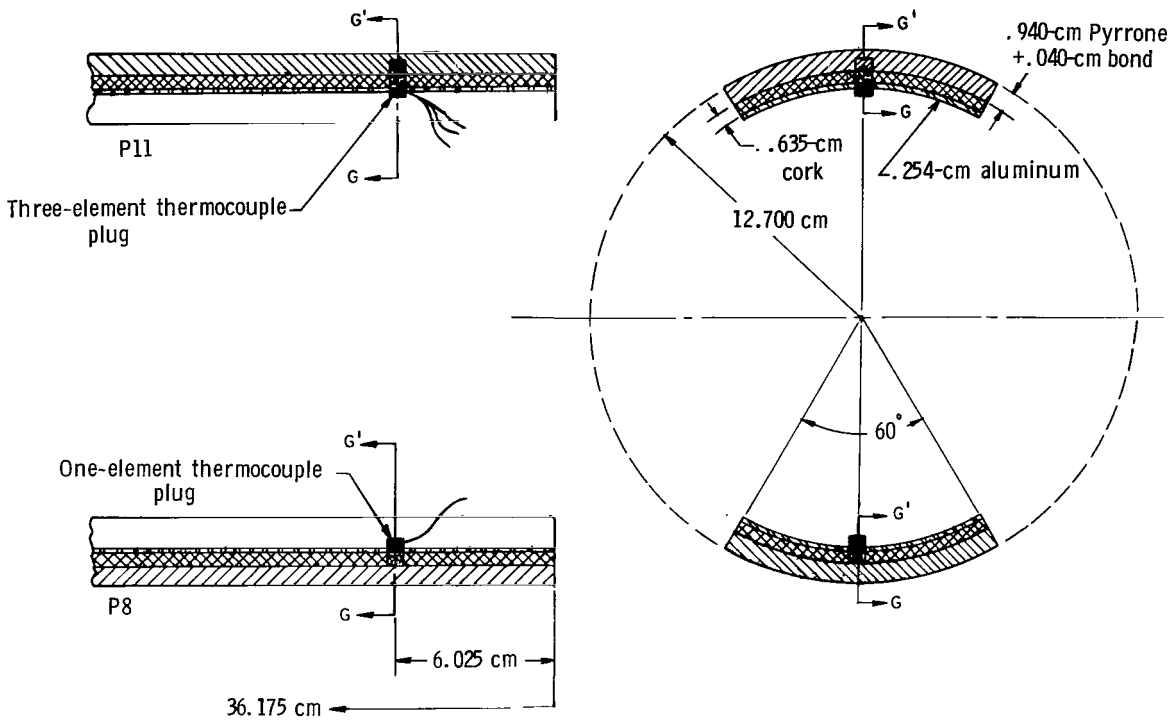

Figure 4.- Sectioned views of flight panels P11 and P8 at station G-G' illustrating thermocouple plugs.

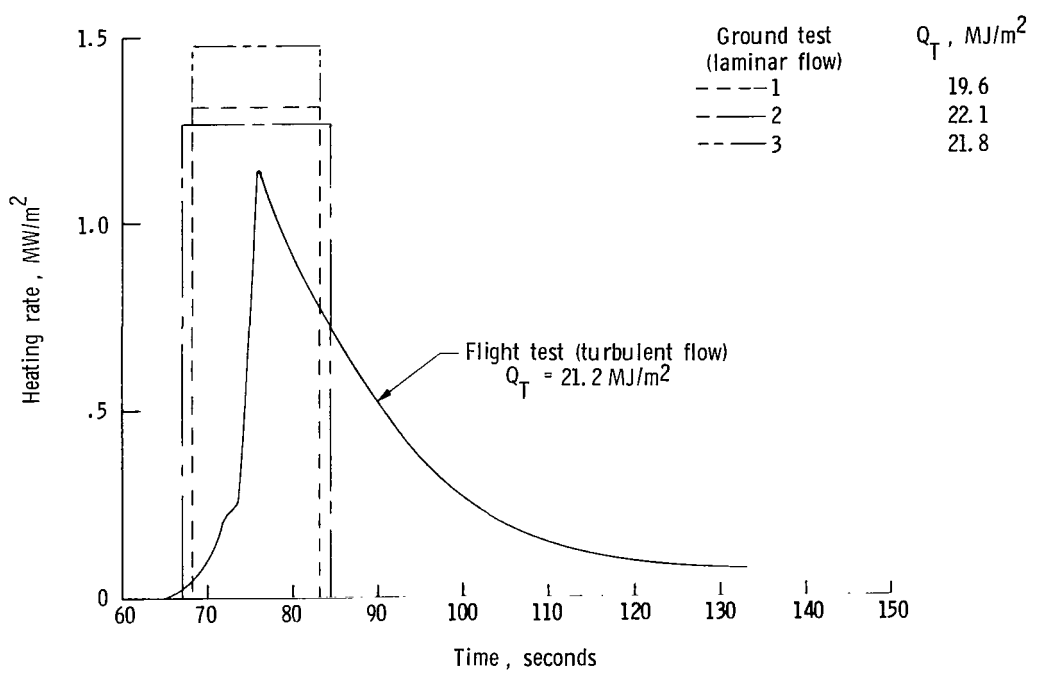

Figure 5.- Comparison of Pacemaker flight-test heating rates at station G-G' with heating rates of special Pacemaker ground tests.

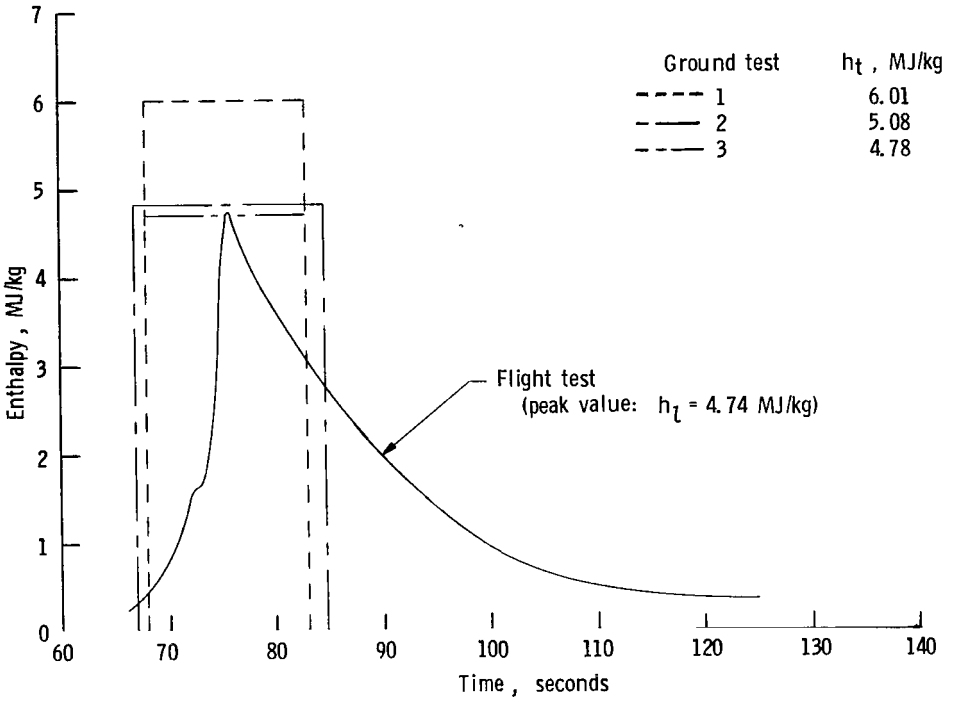

Figure 6.- Comparison of Pacemaker flight-test local-recovery enthalpy at station G-G' with stagnation enthalpies of special Pacemaker ground tests.

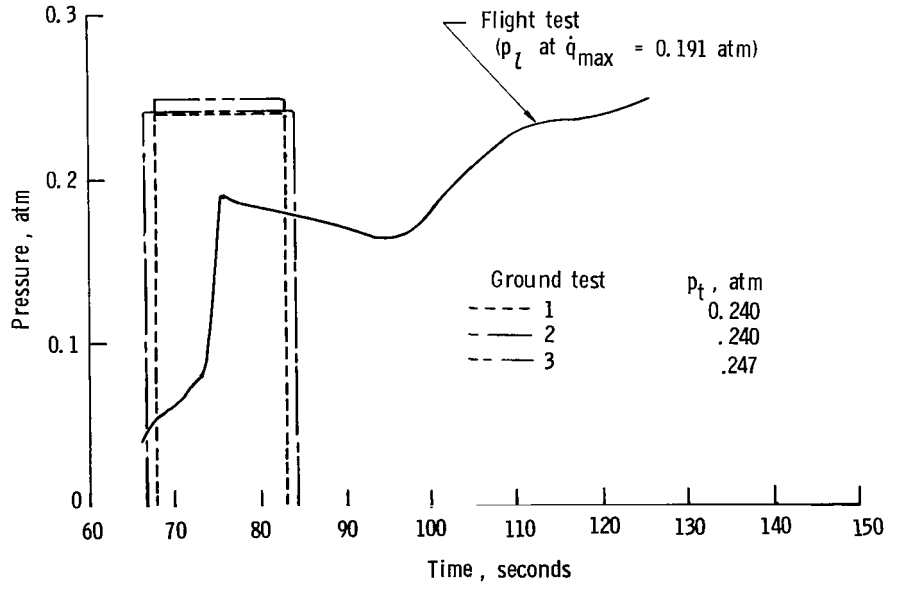

Figure 7.- Comparison of Pacemaker flight-test pressure at station G-G' with pressure levels of the special Pacemaker ground tests.

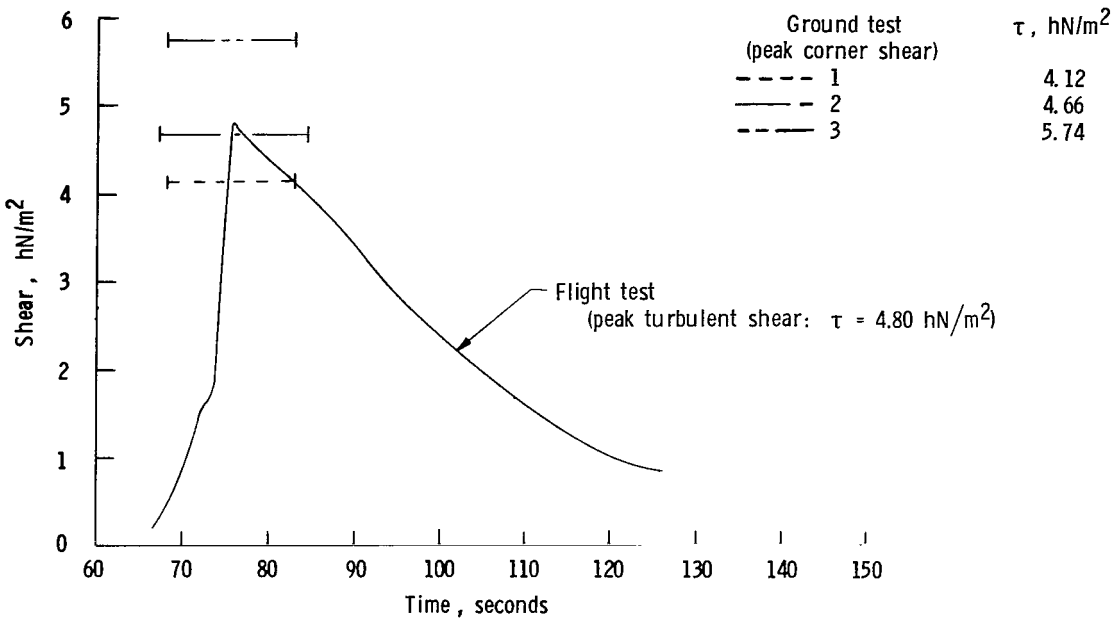

Figure 8.- Comparison of Pacemaker flight-test shear at station G-G' with peak corner shears for special Pacemaker ground tests.

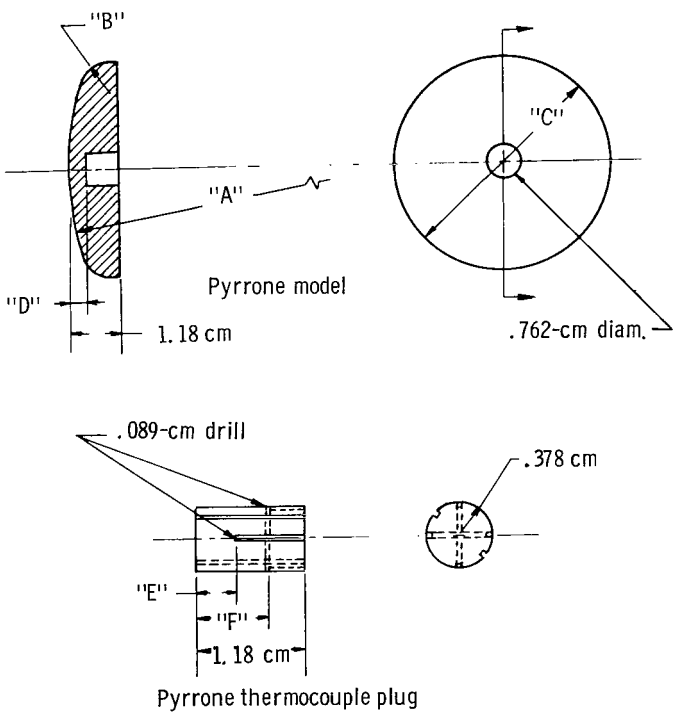

Dimension	Measurement, cm	Material
A	7.82 5.87 3.91	P30 or P60
B	0.695 .518 .348	P30 or P60
C	4.98 3.73 2.49	P30 or P60
D	0.381 .406 .191	P30 P60 P60
E	0.431 .185 .215	P30 P60 P60
F	0.800 .610 .400	P30 P60 P60

Figure 9.- Dimensions of the various test-model bodies and thermocouple plugs.

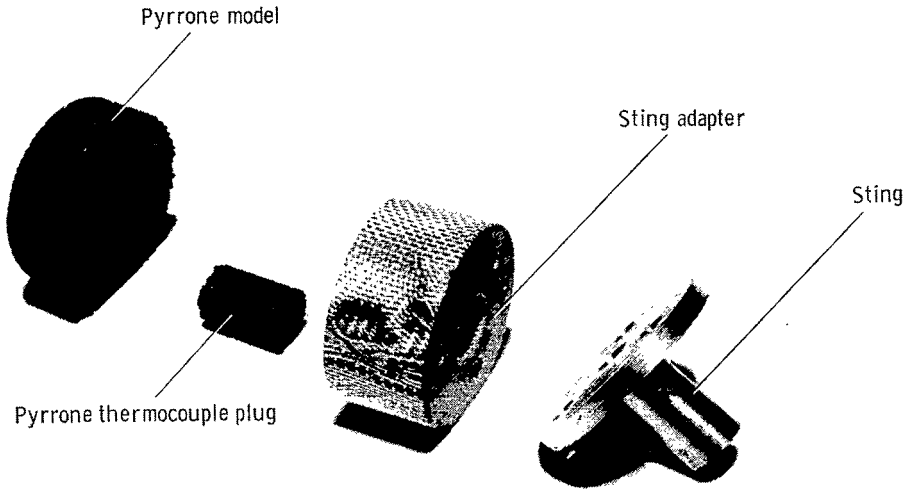

L-68-8056.1

Figure 10.- Typical disassembled ground-test model showing component parts.

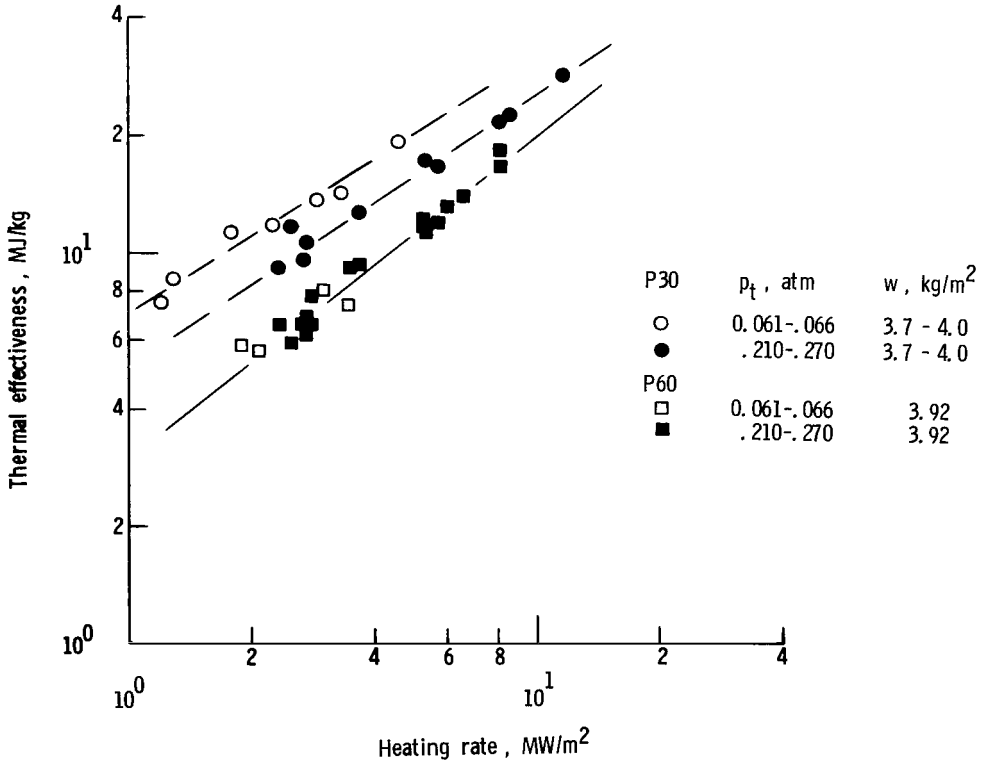

Figure 11.- Comparison between P30 and P60 material thermal-effectiveness values over a range of heating rates.

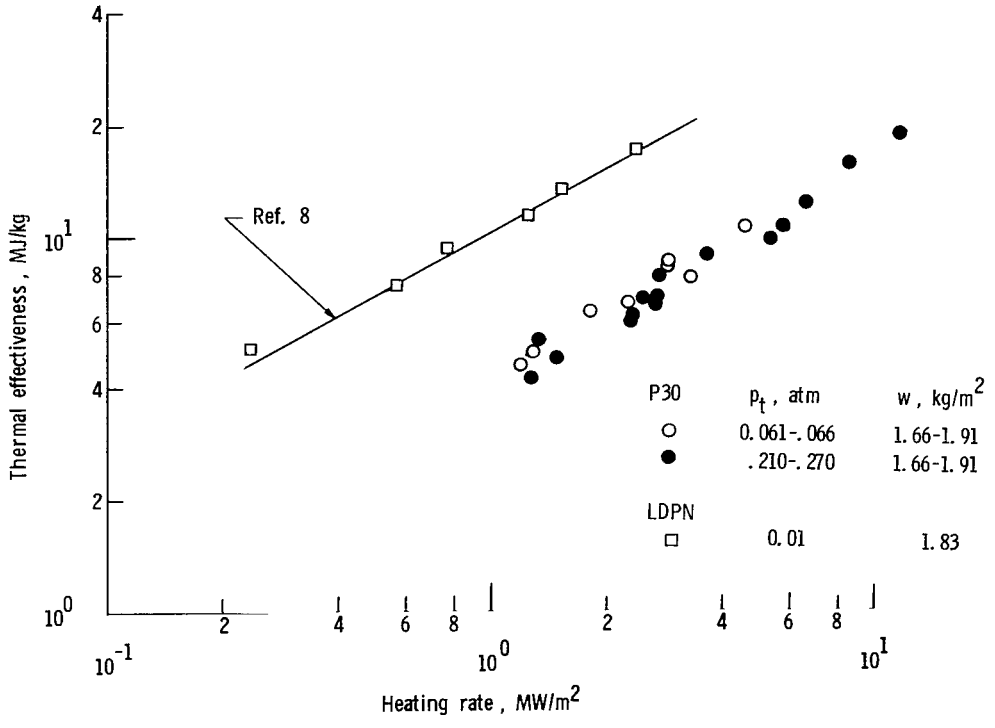

Figure 12.- Comparison of thermal-effectiveness values of low-density phenolic nylon (LDPN) from reference 8 with those of the P30 material.

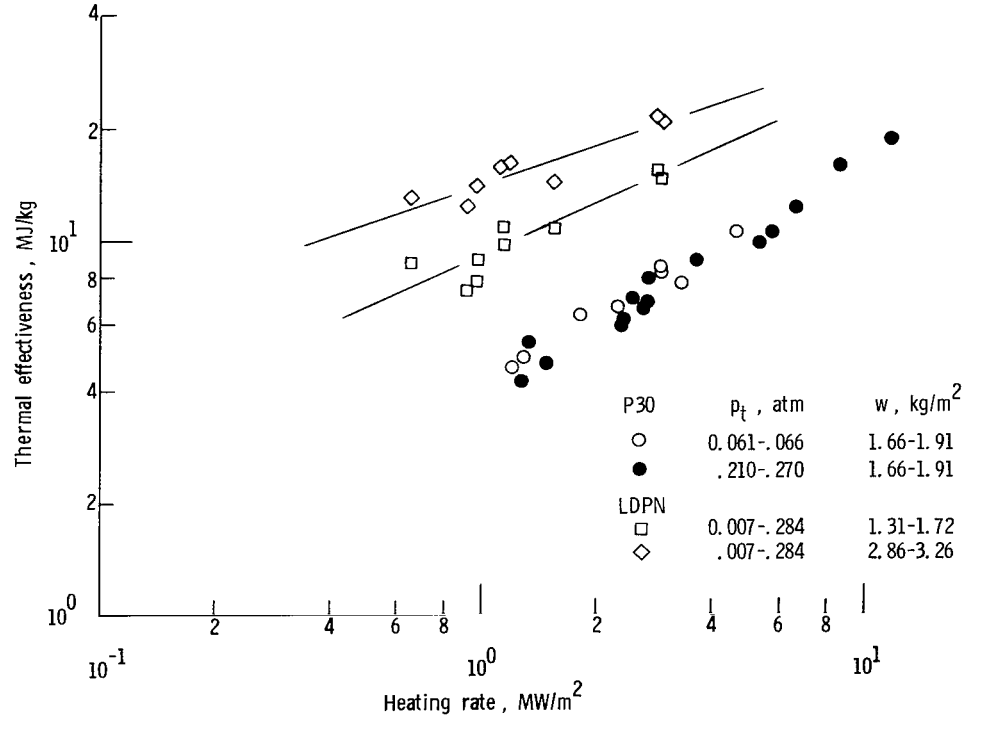

Figure 13.- Comparison of thermal-effectiveness values of low-density phenolic nylon (LDPN) from reference 9 with those of the P30 material.

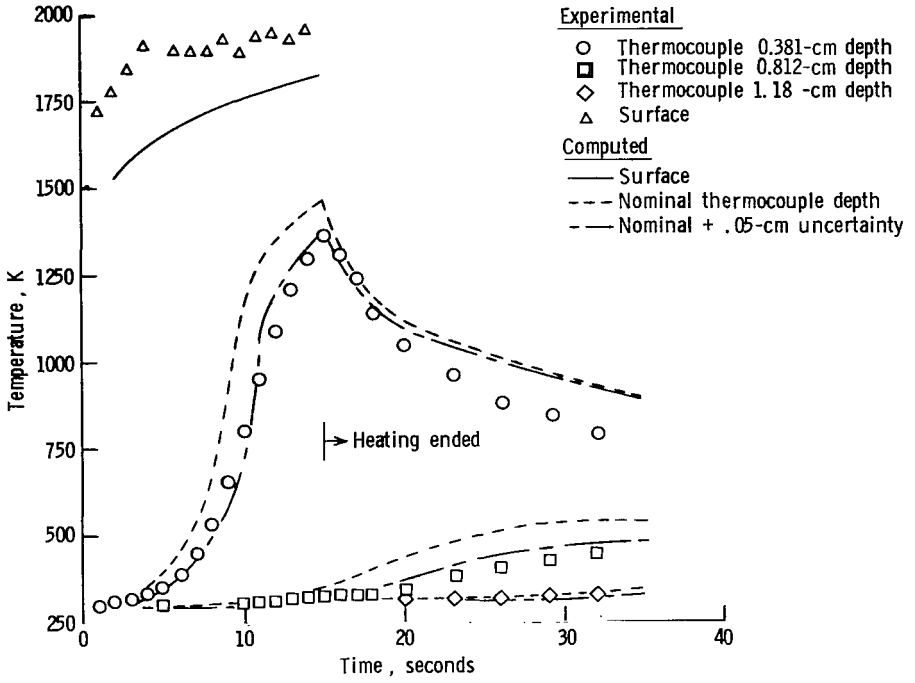

Figure 14.- Computed and measured temperature histories for special Pacemaker ground test 1.

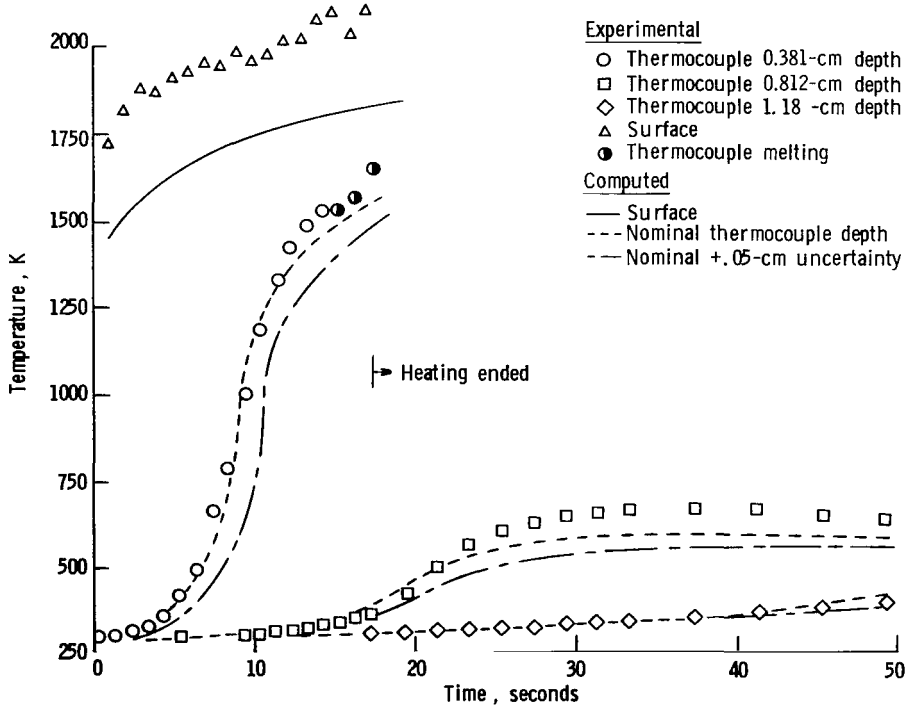

Figure 15.- Computed and measured temperature histories for special Pacemaker ground test 2.

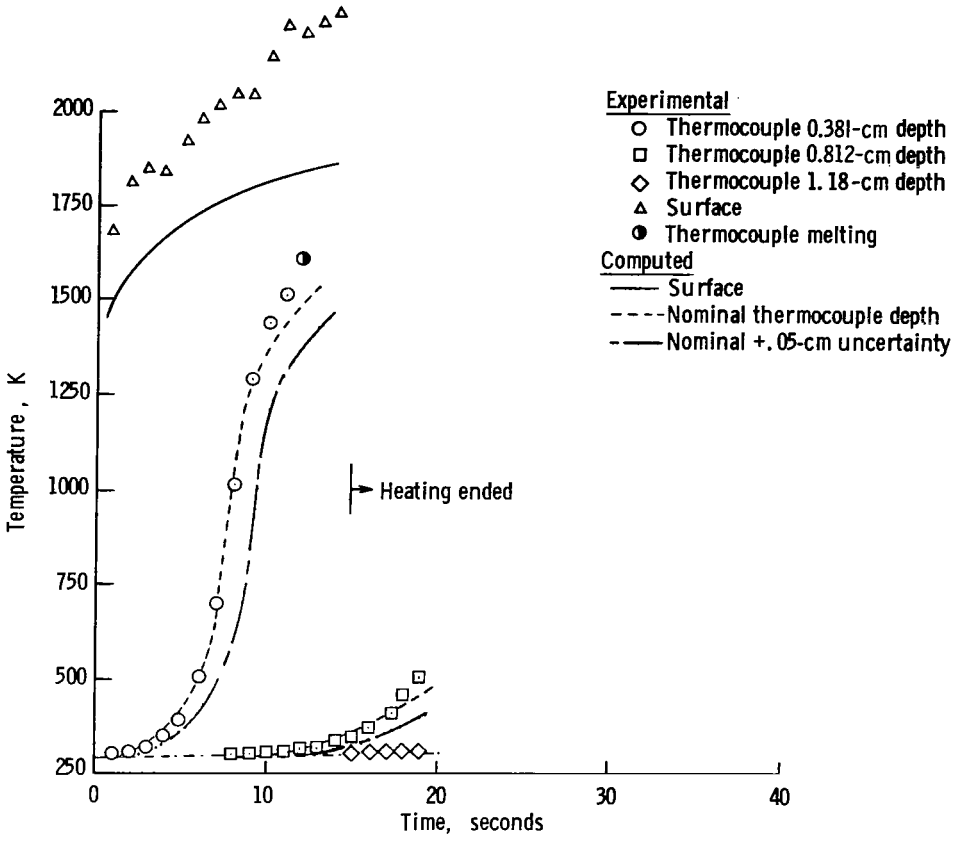

Figure 16.- Computed and measured temperature histories for special Pacemaker ground test 3.

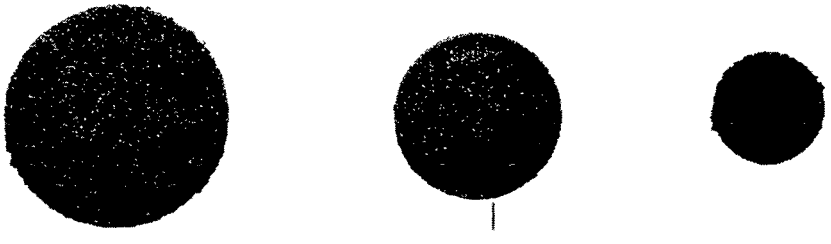

(a) Top view of models.

L-72-143

(b) Sectioned view of models illustrating char-uncharred material interface.

Figure 17.- Top and sectioned views of models from special Pacemaker test vehicle.

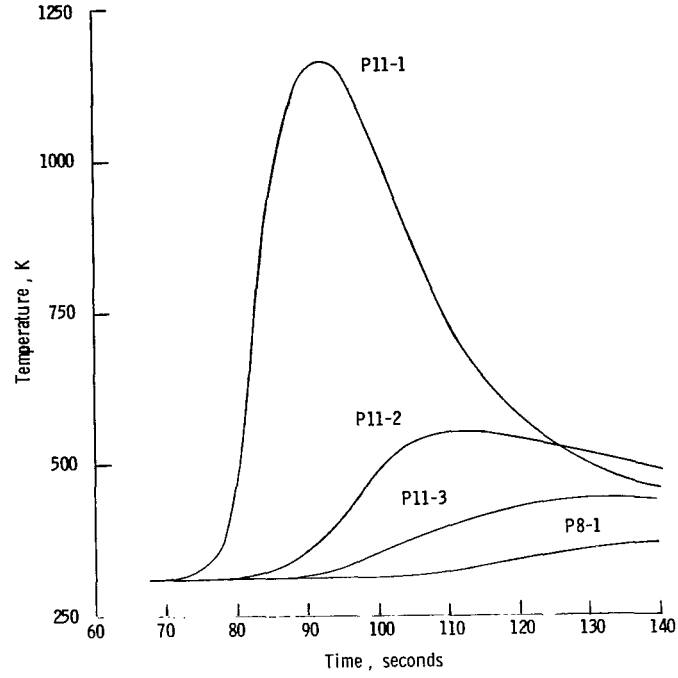

Figure 18.- Measured temperature histories in panels P11 and P8 during the Pacemaker flight.

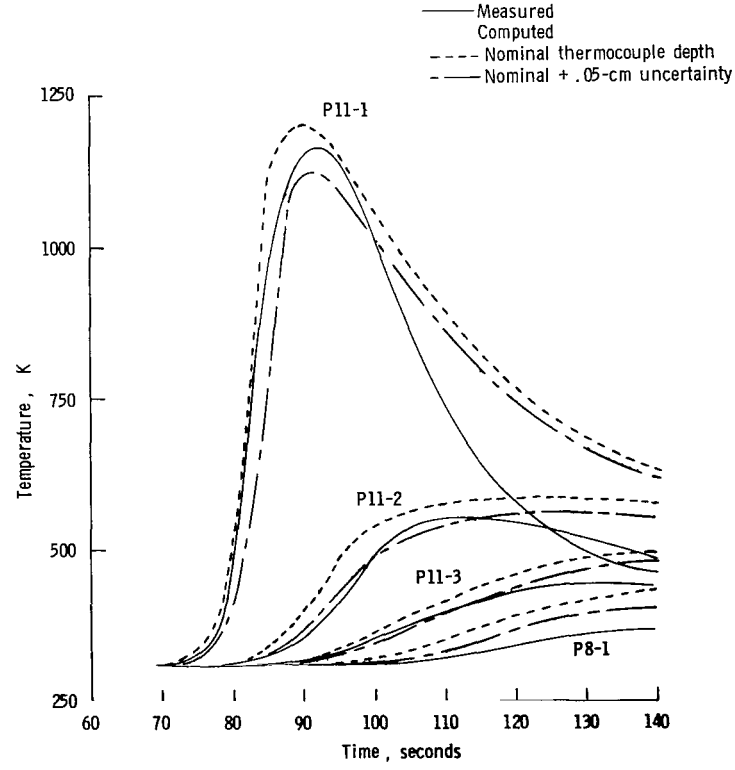

Figure 19.- Comparison between the computed and measured temperature histories for the Pacemaker flight.

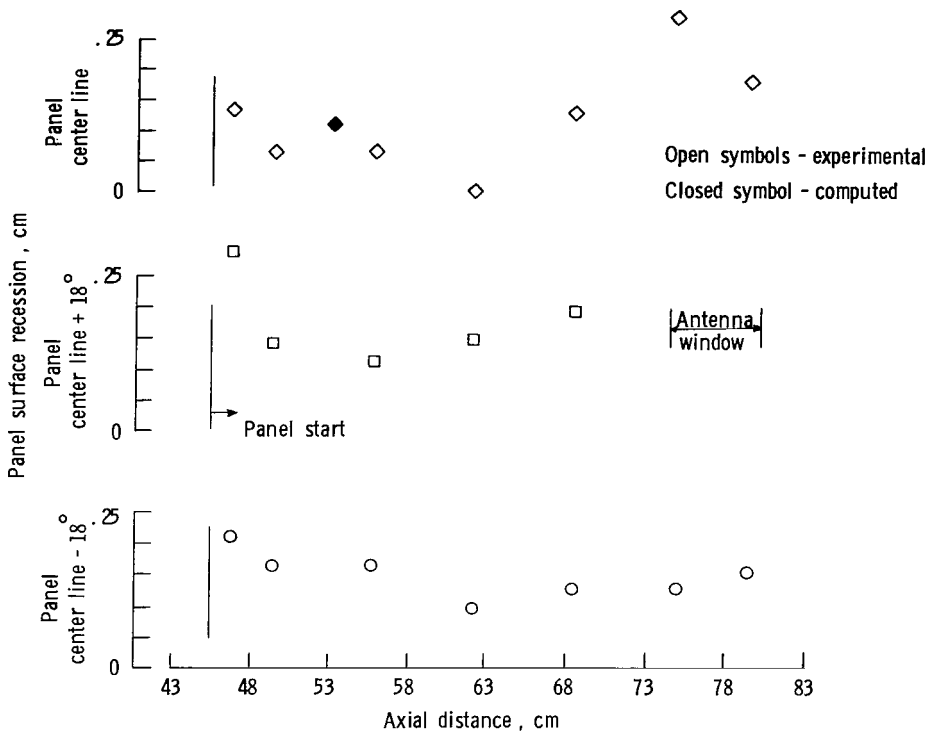

Figure 20.- Computed and measured surface recession of the Pacemaker flight panel designated P11.

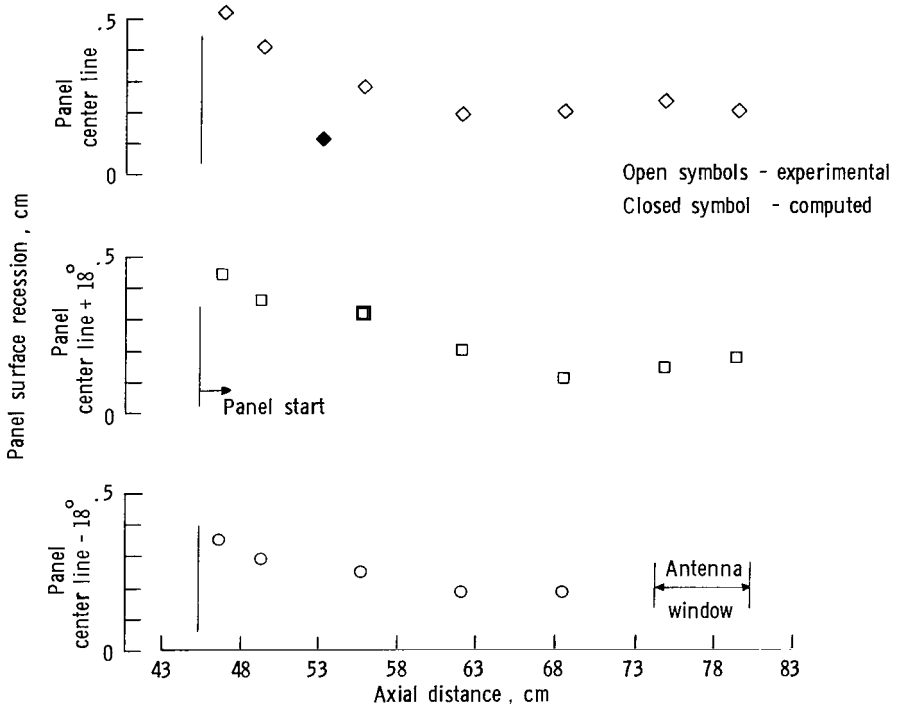

Figure 21.- Computed and measured surface recession of the Pacemaker flight panel designated P8.

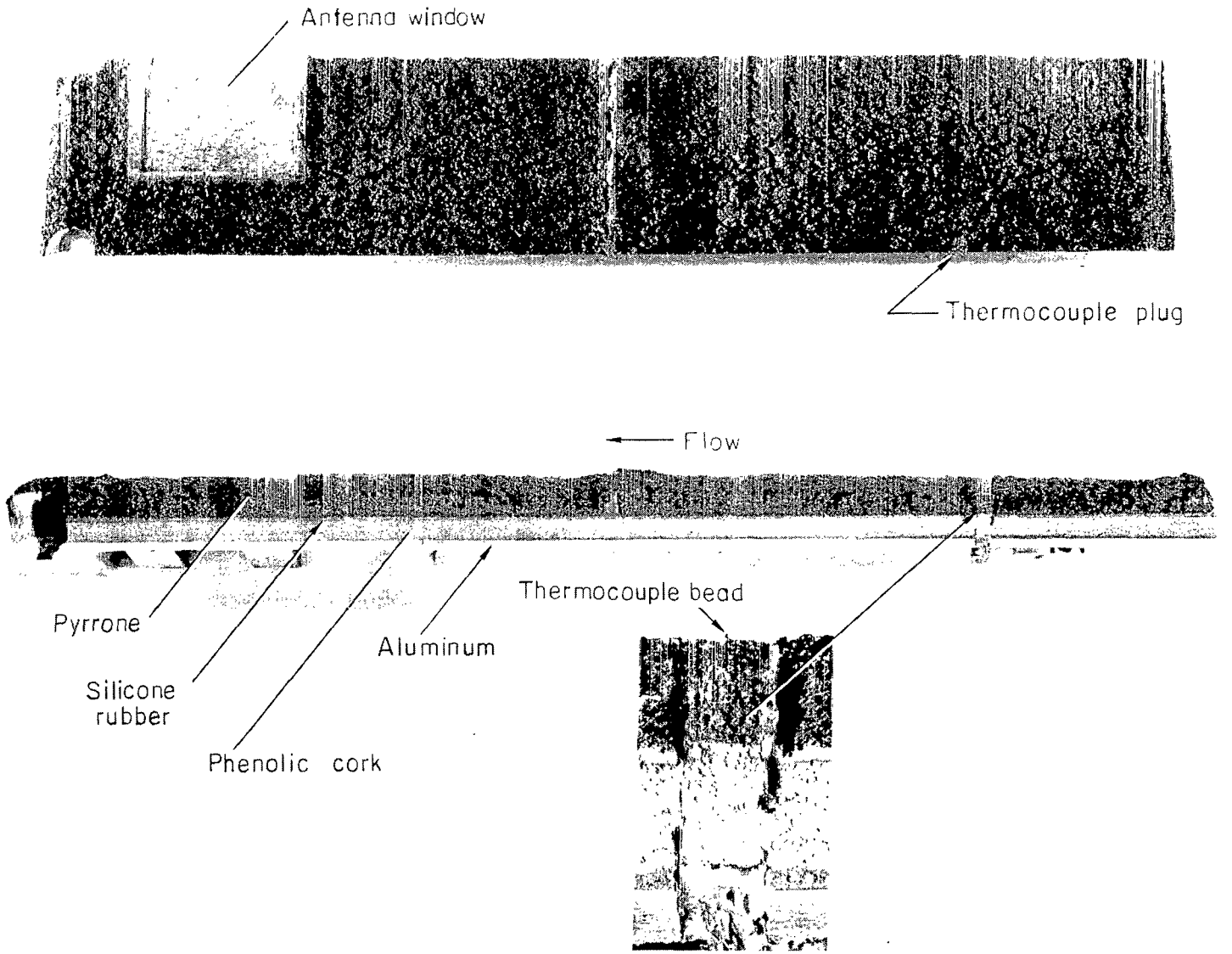

L-72-144

Figure 22.- Postflight top and sectioned view of Pacemaker panel P11 with a closeup of the thermocouple plug.

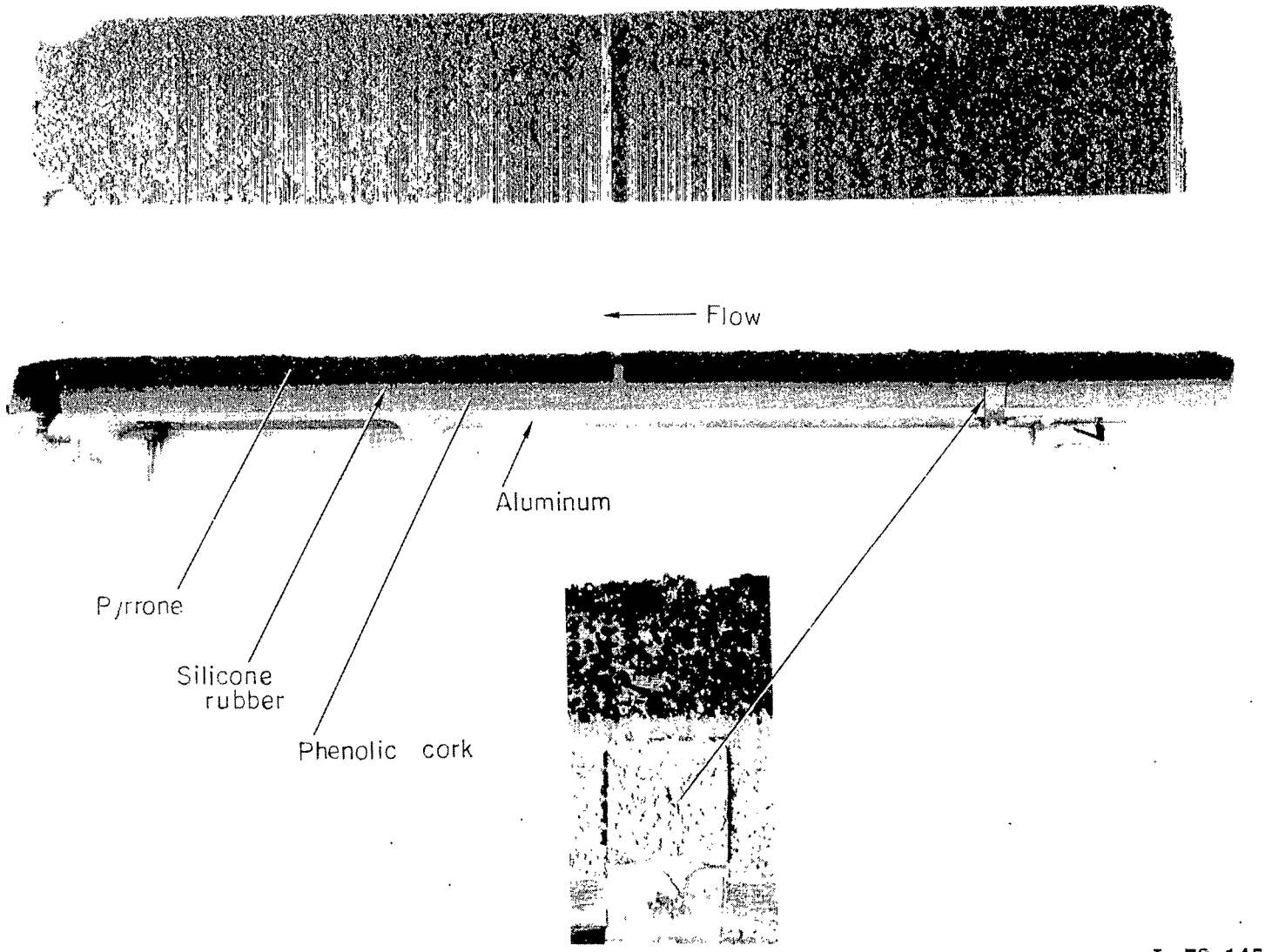

Figure 23.- Postflight top and sectioned view of Pacemaker panel P8 with a closeup of the thermocouple plug.

"The aeronautical and space activities of the United States shall be conducted so as to contribute . . . to the expansion of human knowledge of phenomena in the atmosphere and space. The Administration shall provide for the widest practicable and appropriate dissemination of information concerning its activities and the results thereof."

—NATIONAL AERONAUTICS AND SPACE ACT OF 1958

NASA SCIENTIFIC AND TECHNICAL PUBLICATIONS

TECHNICAL REPORTS: Scientific and technical information considered important, complete, and a lasting contribution to existing knowledge.

TECHNICAL NOTES: Information less broad in scope but nevertheless of importance as a contribution to existing knowledge.

TECHNICAL MEMORANDUMS: Information receiving limited distribution because of preliminary data, security classification, or other reasons.

CONTRACTOR REPORTS: Scientific and technical information generated under a NASA contract or grant and considered an important contribution to existing knowledge.

TECHNICAL TRANSLATIONS: Information published in a foreign language considered to merit NASA distribution in English.

SPECIAL PUBLICATIONS: Information derived from or of value to NASA activities. Publications include conference proceedings, monographs, data compilations, handbooks, sourcebooks, and special bibliographies.

TECHNOLOGY UTILIZATION PUBLICATIONS: Information on technology used by NASA that may be of particular interest in commercial and other non-aerospace applications. Publications include Tech Briefs, Technology Utilization Reports and Technology Surveys.

Details on the availability of these publications may be obtained from:

SCIENTIFIC AND TECHNICAL INFORMATION OFFICE

NATIONAL AERONAUTICS AND SPACE ADMINISTRATION

Washington, D.C. 20546